TABLE 2 Composition of glass shards from Levantine and Black Sea cores

Core	Number of shards	Na_2O	MgO	Al_2O_3	SiO_2	P	S	K_2O	CaO	TiO_2	MnO	FeO*	Cl
TRI172-22	10	4.99	0.12	13.61	73.02	0	0.17	3.37	1.4	0.3	0.11	2.13	0.78
		(0.46)	(0.13)	(0.21)	(0.47)	(0.01)	(0.12)	(0.16)	(0.15)	(0.14)	(0.13)	(0.25)	(0.13)
GGC-79	16	5.01	0.23	13.69	72.93	0.01	0.19	3.33	1.33	0.32	0.07	2.08	0.8
		(0.28)	(0.12)	(0.28)	(0.56)	(0.02)	(0.13)	(0.11)	(0.1)	(0.1)	(0.07)	(0.22)	(0.1)
Minoan	141	4.9	0.26	13.7	72.5	n.i.	n.i.	3.1	1.3	0.26	n.i.	1.9	n.i.
			(0.02)	(0.4)	(1.1)			(0.2)	(0.1)	(0.1)		(0.1)	
Minoan (Bo)	6		0.24	13.6	70.6	n.i.	n.i.	3.12	1.35	0.26	n.i.	1.74	n.i.
			(0.02)	(0.06)	(0.18)			(0.04)	(0.01)	(0.02)		(0.06)	

Shards from Minoan tephra in Levantine core TRI172-22 and in Black Sea core GGC-79. For GGC-79 the ash layer was carefully sampled, an oily fraction was discarded by methanol, the sample was washed with water, sieved at 25 μm and dried, then individual glass shards were picked for electron microprobe analysis. Major element analyses were made on individual glass shards with a scanning electron microscope, coupled with an energy-dispersive X-ray spectrometer. Standard deviation (2σ) in parenthesis. FeO: total iron expressed as FeO. Minoan data refers to marine tephra layers of Minoan age from eastern Mediterranean area[24]. Minoan (Bo) refers to land deposit on Santorini island ("upper pumice serie")[24]. n.i.: no information.

Therefore, we propose to use the mean ^{14}C age from the ash layer of the two cores, and to consider age difference of 1,285±460 yr between this and the Minoan event as representative of the inferred ^{14}C age of Black Sea surface waters at the time of deposition.

It is inappropriate to assume the same $\Delta^{14}C$ correction for a mid-latitude open ocean site (~ 400 yr)[17] and a nearly closed basin such as the Black Sea. Moreover, the calibration of 1,285±460 yr which we infer for Black Sea surface water at 3,355 yr BP is in good agreement with the pre-bomb age of about 1,430 yr for surface water estimated from a three-box model[31]. The Black Sea circulation was presumably close to steady state well before the Minoan outburst at 3,355 yr BP. The start of the Mediterranean input occurred between 7,000 and 12,000 yr BP[8,9,15]; it then took 2,000 yr or less before all the previous deep water was exchanged[32]. Therefore, the inferred $\Delta^{14}C$ correction of ~ 1,280 yr is applicable over the past several thousand years since the renewal of deep water was completed.

This study underlines the delicate use of ^{14}C data in the Black Sea stratigraphy. The Minoan horizon, extending eastwards over a large part of Asia Minor from its source, provides an important calibration horizon for the chronology of recent Black Sea sediments. □

Received 13 April 1992; accepted 6 April 1993.

1. Marinatos, S. *Antiquity* **13**, 425–439 (1939).
2. Manning, S. W. in *Thera and the Aegean World III* (ed. Hardy, D. H.) 29–41 (Thera Foundation, London, 1990).
3. Kunilholm, P. I. in *Thera and the Aegean World III* (ed. Hardy, D. H.) 13–18 (Thera Foundation, London, 1990).
4. Watkins, N. D., Sparks, R. S. J., Sigurdsson, H., Huang, T. C. & Federman, A. *Nature* **271**, 122–126 (1978).
5. Sparks, R. S. J. & Wilson, C. J. N. in *Thera and the Aegean World III* (ed. Hardy, D. H.) 89–99 (Thera Foundation, London, 1990).
6. Sigurdsson, H., Carey, S. & Devine, J. in *Thera and the Aegean World III* (ed. Hardy, D. H.) 100–112 (Thera Foundation, London, 1990).
7. Pyle, D. in *Thera and the Aegean World III* (ed. Hardy, D. H.) 113–121 (Thera Foundation, London, 1990).
8. Ross, D. A., Degens, E. T. & MacIlvaine, J. *Science* **170**, 163–165 (1970).
9. Ross, D. A. & Degens, E. T. in *The Black Sea: Geology, Chemistry and Biology* (eds Ross, D. A. & Degens, E. T.) 183–199 (Am. Assoc. Pet. Geol. Mem., 1974).
10. Degens, E. T. *et al. Neues Jb. Geol. paläeontol. Monat.* **5**, 65–86 (1980).
11. Calvert, S. E., Karlin, R. E., Toolin, L. J., Donahue, D. J. & Southon, J. R. *Nature* **350**, 692–695 (1991).
12. Jones, G. A. *Radiocarbon* **33**, 211–213 (1991).
13. Crusius, J. & Anderson, R. F. *Paleoceanography* **7**, 215–227 (1992).
14. Crusius, J. & Anderson, R. F. *Geochim. cosmochim. Acta* **55**, 327–333 (1991).
15. Hay, B. J., Arthus, M. A., Dean, W. E., Neff, E. D. & Honjo, S. *Deep-Sea Res.* **38**, Suppl. 2A, S1211–S1235 (1991).
16. Friedrich, W., Wagner, P. & Tauber, H. in *Thera and the Aegean World III* (ed. Hardy, D. H.) 188–196 (Thera Foundation, London, 1990).
17. Bard, E. *Paleoceanography* **3**, 635–645 (1988).
18. Calvert, S. E. & Fontugne, M. R. *Chem. Geol. (Isotope Geosci. Section)* **66**, 315–322 (1987).
19. Innocenti, F., Mazzuoli, R., Pasquare, G., Radicati di Brozolo, F. & Villari, L. *Geol. Mag.* **112**, 349–360 (1975).
20. Keller, J. in *Tephra Studies* (eds Self, R. S. J. S. & Sparks, S.)227–244 (Reidel, Dordrecht, 1981).
21. Keller, J., Rehren, T. H. & Stadlbauer, E. in *Thera and the Aegean World III* (ed. Hardy, D. H.) 13–26 (Thera Foundation, London, 1990).
22. Paterne, M., Guichard, F., & Labeyrie, J. *J. Volcan. geotherm. Res.* **34**, 153–172 (1988).
23. Calvert, S. E., Vogel, J. S. & Southon, J. R. *Geology* **15**, 918–921 (1987).
24. Federman, A. N. & Carey, S. *Quat. Res.* **13**, 160–171 (1980).
25. Innocenti, F., Mazzuoli, R., Pasquare, G., Serri, G. & Villari, L. *Geol. Rundsch.* **69**, 292–322 (1980).
26. Aydar, E. *Les Laves du Quaternaire de Cappadoce (Turquie): Volcanologie et Petrologie* (Mémoire DEA, Clermont-Ferrand Univ. 1989).
27. Pearce, J. A. *et al. J. Volcan. geotherm. Res.* **44**, 189–229 (1990).
28. Woods, A. W. & Wohletz, K. *Nature* **350**, 225–227 (1991).
29. Stanley, D. J. & Sheng, H. *Nature* **320**, 733–735 (1985).
30. Jouanneau, J.-M. *Mar. Chem.* **21**, 189–197 (1987).
31. Murray, J. W., Top, Z. & Ozsoy, Z. *Deep-Sea Res.* **38**, suppl. 2A, S663–S689 (1991).
32. Boudreau, B. P. & Leblond, P. H. *Paleoceanography* **4**, 157–166 (1989).
33. Sullivan, D. G. *Nature* **333**, 552–554 (1988).
34. Honjo, S. *et al. Cruise Rep. R. V. Knorr 138–4, Leg 1 April 16–May 17, 1988;* and *Piri Reis Int. Contrib. Series No.6.* (1988).

ACKNOWLEDGEMENTS. This work was begun by F. G. during a stay at the Graduate School of Oceanography which was supported by a NATO grant. We also thank the French Commissariat à l'Energie Atomique, the CNRS and the Woods Hole Oceanographic Institution for making sample collection possible. The core curation of the URI-GSO collection is supported by the NSF (for sampling of core TRI172–22). This work benefited from help and discussion with I. Bentaled, E. Boyle, J. Broda, H. Cachier, S. Calvert, J.-C. Duplessy, M. Fontugne, P.-Y. Gillot, A. Gourgaud, C. Laj, C. Lalou, E. Neff, M. Paterne and J. Quinn.

Estimate of pyroclastic flow velocities resulting from explosive decompression of lava domes

Jonathan H. Fink & Susan W. Kieffer

Geology Department, Arizona State University, Tempe, Arizona 85287-1404, USA

APPARENTLY benign silicic domes or lava flows can travel for several kilometres and then suddenly collapse to generate pyroclastic phenomena capable of causing widespread destruction, as happened recently at Mount Unzen in Japan[1]. Two sources have been proposed for the energy that propels such 'Peléan' or 'Merapi'-type[2] pyroclastic flows: gravitational collapse (supplemented by heating and expansion of air) and sudden expansion of pressurized gases from inside the lava flow. If gravity controls the energy transfer, then areas likely to be affected can be predicted on the basis of topography[3], and the resulting deposits will bear a simple relationship to the part of the lava flow from which they issued. But if gas pressure adds a significant contribution, hazard assessment becomes more difficult because gas decompression adds velocities beyond those

acquired by gravitational forces, putting much larger areas at risk and forming pyroclastic deposits that are much more difficult to relate to their source. Here we estimate the initial velocities of pyroclastic flows generated by dome disintegration for a range of lava compositions and volatile contents, and offer a conceptual framework for correlating the dynamics of dome-front collapse with the resulting sediment record. Our results indicate that explosive decompression at distal portions of domes can cause velocities comparable to gravitational collapse, especially in cases where volatiles become locally concentrated above equilibrium values.

We focus on those relatively gas-poor ($[H_2O]<1.0$ wt%) pyroclastic flows known as block-and-ash flows and associated surges, in contrast to the more gas-rich pumice and ash flows or ignimbrites that result from collapsing eruption columns. Although there are several detailed theoretical models for collapse of gassy eruption clouds directly over a primary eruptive vent[4–6], and other studies containing direct and indirect observational evidence of lava dome disintegration[7,8], we are not aware of any quantitative models for the ways in which the front of a lava dome may transform itself into a pyroclastic flow. (Although lava domes and lava flows may be considered part of a morphological continuum, here for brevity we refer to both as lava domes.) Here we compare two endmember cases: (1) gravitational collapse of the front of a lava dome with initial velocities determined solely by conversion of potential energy into kinetic energy as pieces tumble to the ground[9,10]; and (2) explosive emission of gas and rock from the flow front after exposure of lava at high pressure to ambient pressure by sudden removal of covering material[7,11–13]. Gas-dynamic effects associated with endmember (2) can be large at early times, and it is this influence that we examine.

We rely on recent numerical models of large volcanic debris avalanches to estimate the maximum velocities due to gravity, and assume that the rheological and dynamic behaviour of collapsing domes and volcanic landslides will be similar because both are made up largely of hot blocks of lava. Calculated and observed velocities for the avalanches that flowed down the Toutle river valley at the onset of the 18 May 1980 eruption of Mount St Helens are typical of several other landslides[14]. For a range of rheological parameters, velocities were about 10 m s^{-1} for the first 10 s of flow, increasing up to 150 m s^{-1} at 30 – 60 s as the avalanche accelerated downslope. These values will be used below for comparison with decompression effects.

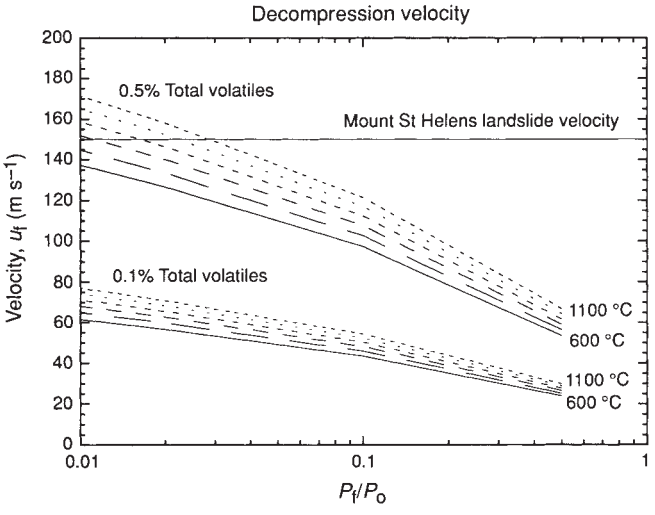

FIG.1 Plot of velocities of pyroclastic particles generated by collapse of lava dome fronts for a range of total volatile contents, internal pressures and temperatures. Highest values are comparable to those generated by gravitational collapse.

To first order, the violence of the emission of gas and rock from the front of a lava dome when covering material has been suddenly removed depends on the ratio of pressure of the gas within the dome (P_o is the sum of lithostatic pressure and strength) to that in the atmosphere (P_f); the average initial temperature (T_o); and the gas to rock ratio (x). The problem is a difficult one of unsteady, multi-component (rock, water vapour, CO_2 and so on), multiphase (gas, liquid, solid), non-equilibrium (separated) flow. Because of limitations in available data, we used measured water content, but a more detailed analysis would use total exsolved gas. The analysis below ignores many of the complicating factors, but illustrates that the magnitude of the decompression effect can approach that due to gravity.

A minimum value for initial pressure in collapsing lava domes is the lithostatic load of a few bars to a few tens of bars, but internal pressure is also influenced by the strength of the lava. Although the upper surfaces of active lava domes appear blocky and fragmented, the inward increase in temperature means that there is some depth below which the lava remains molten and ductile[15]. Strengths of glassy obsidian measured in the laboratory[16] are generally of the order of 0.1 MPa. Models for deformation of the Mount St Helens dacite dome[17,18] yield estimates of the strength of the surface crust between about 0.1 and 10 MPa.

The amount of energy available during decompression also depends on the volatile content of the lava, which typically ranges from water values of 0.1 wt% for rhyolites to 0.4 for andesites[19]. Equally large variations can be found within a single extrusion, depending on emplacement sequence and vesicularity. At the Mount St Helens dacite dome, individual lobes had water contents that increased regularly from the flow front (typical values near 0.1 wt%) to the vent (0.3 – 0.4 wt%)[20]. Dacite from the active Santiaguito dome in Guatemala has measured water contents ranging from 0.03 to 0.25 wt%[21]. In drill cores through one of the young Inyo rhyolite flows[22,23] water contents ranged from 0.1 to 0.45 wt% with the highest concentrations found exclusively in glassy septa within coarsely vesicular zones located 15–20 m below the flow surface[24,25]. These relations and petrographic evidence suggest that the water-rich zones result from migration and concentration of volatiles beneath a nondeforming carapace[11,15] possibly supplemented by crystallization of anhydrous minerals in the flow interior[12].

Measured and estimated eruption temperatures for silicic lavas range between about 600 and 1,100 °C (ref.16). During advance of a lava dome, the surface temperature may drop to ambient levels but the interior, insulated by the blocky and vesicular carapace, should maintain temperatures near the eruption range for months to years[26,27].

From these data, in the calculations below we will assume the following bracketing values for properties of lava domes of rhyolite to andesite composition: P_o=0.1–3.0 MPa; x=0.1–0.5 wt% and T_o=600–1,100 °C.

Our mathematical model for expansion of a pressurized lava dome involves many assumptions, of which the most severe are these. First, the expanding pyroclastic flow is considered to be homogeneous (in the fluid dynamical sense that there is no separation between the gas and the particles), and second, particle–particle interactions are neglected. The first assumption implies that initially the gas expansion 'instantaneously' accelerates the entrained particles up to the exit velocity, a limit approached only for particles much smaller than many of those found in block-and-ash flows. The second assumption is a serious restriction; at present there is no theoretical framework allowing rigorous consideration of 'granular' flow admixed with compressible gases. We estimate that these simplifications could cause the calculated velocities to exceed those obtained by fragments in a pyroclastic flow by a factor of two to three. Offsetting this effect, however, is the gas-phase separation at high velocities which will be discussed below.

Let us consider a volume of material at the front of the lava dome to be described by the thermodynamic parameters P_o, T_o, x (weight fraction of total exsolved volatiles, assumed here to be H_2O), and velocity u_o (=0 in the initial state). We assume that the flow front suddenly collapses and that the dusty gas mixture expands rapidly (adiabatically and isentropically) to a final pressure P_f (taken to be atmospheric pressure, 0.1 MPa). The process is further constrained to be one-dimensional, isothermal and frictionless, and the initial pressure P_o is assumed to be at least two to three times atmospheric.

We calculate the final velocity, u_f, by deriving an equation of state and an adiabatic expansion law for the dense mixture. The method of solution follows that for an inviscid pseudo-gas[28]. Our derivation demonstrates that thermodynamically the mixture can be treated as a perfect gas with the gas constant, R, modified to account for the composition of the gas phase(s) and the mass-loading of solids; with the isentropic exponent γ, modified to account for the heat transfer; and with the volume modified to account for the presence of the solid phase. The quantity of interest is the velocity obtained on decompression, given by the St Venant–Wantzel equation:

$$u_f = \{2\gamma RT[(1-P_f/P_o)/(\gamma-1)\}^{1/2}$$

The equation gives the maximum speed attainable by a pseudo-gas that expands isentropically from an infinite reservoir[29]. In a real gas, friction reduces the obtainable velocity.

For H_2O vapour, R_{H_2O} is 0.46×10^7 erg K^{-1} g^{-1}, C_P is 4.19 J $g^{-1}K^{-1}$, and C_V is 3.14 J $g^{-1}K^{-1}$. For typical solid fragments, the specific heat capacity C_s = 1.00 J $g^{-1}K^{-1}$. Using these values, and for x=0.1–0.5%; T=600–1,100 °C; and pressure ratios P_f/P_o = 0.03–1, we derive the values of plausible velocity shown in Fig. 1. The maximum calculated excess velocity for these conditions is 170 m s^{-1} for a lava at an eruption temperature of 1,100 °C, water content of 0.5 wt%, and pressure of 100 bar within the lava dome. Even for more conservative values for a rhyolite flow of 800 °C, 0.4 wt% H_2O, and 10 bar pressure, an excess velocity of over 100 m s^{-1} is produced.

Despite uncertainties in the model, it is clear that gas pressure is capable of propelling pyroclastic material to velocities comparable to those for gravity alone, and the gas–dust fraction may travel even faster. Because gas at high pressures expands laterally on decompression, the area over which such high velocities would occur will be broader and more difficult to predict than those affected by gravitational collapse alone. If gassy blocks tumble from the front of a flow or are crushed in transit, local high-velocity gas emissions may also occur[8].

Much of our knowledge of these endogenic explosive phenomena must be gleaned from analysis of the resulting pyroclastic deposits. If simple gravitational collapse occurs, deposits should resemble landslide deposits in texture and be confined to areas limited by potential energy conversion and energy dissipation. In contrast, gas-driven decompression may produce a variety of deposits, and can be driven outwards or upwards beyond gravitationally determined limits by conversion of stored enthalpy to kinetic energy[13]. Some ideas about the relation between gas decompression and resulting deposits are shown in Fig. 2.

The front of a dome is assumed to fall off, for example by oversteepening, at x=0, t=0 (upper left of Fig. 2). As shown in the main part of the figure, this sudden exposure of the dome's interior to ambient pressure results in a complex decompression wave which would be called a rarefaction wave in simple gas dynamics. However, this decompression is probably much more complex in dome failure with expansion and acceleration of free volatile phases, nucleation and growth of dissolved volatiles if kinetics permit, and fragmentation of the liquid or semi-rigid component.

In our calculations, the acceleration of particles and gas is assumed to be homogeneous, but as shown in the figure, there is probably substantial segregation of the gas phase, the fines and the coarse particles. The segregation process could produce different flow regimes (ash hurricanes, surges, block and ash flows) and a variety of depositional facies depending on processes downslope as well as on the initial flow segregation near the dome. The relations may not be simple, depending on relative velocities of the different flow regimes as well as on such factors as slope, channel formation and external water.

In summary, differences in pressure and gas content within lava domes can produce variations in the intensity of pyroclastic phenomena generated by flow-front collapse. Estimating the magnitude of explosive effects thus requires knowledge of the variability of front thickness and lava volatile contents. Increases in lava vesicularity (usually detectable on aerial photographs as a darkening of the lava surface or ballistic expulsion of blocks from the flow surface) may reflect magma volatile content and can serve as warning signs of an enhanced likelihood of explosive decompression. The course of future pyroclastic flows cannot be reliably determined solely by tracing the paths of prior flows generated by collapse of any given lava-dome lobe, nor by noting the elevation of the flow front relative to surrounding topography. In particular, mapped distributions of older block-and-ash deposits probably greatly underestimate the potential devastation zone because they exclude evidence of the less well-preserved gassy parts of previous flows. On the other hand, calculated estimates of decompression velocities can help delineate zones likely to be affected by future volcanic blasts and surges.

Mount Unzen's pyroclastic flow of 3 June 1991, which killed three volcanologists and 40 others, illustrates how poorly the variability of dome processes has been appreciated, even among experts. If this exceptionally destructive flow emanated from a portion of the dome that was even slightly more volatile-enriched, it could have had a considerably higher initial velocity, more vertically extensive ash hurricane cloud, longer runout distance and broader area of impact. Although we will never know, monitoring of the dome surface might have revealed changes in lava texture or fumarole activity and helped to avert the tragedy. □

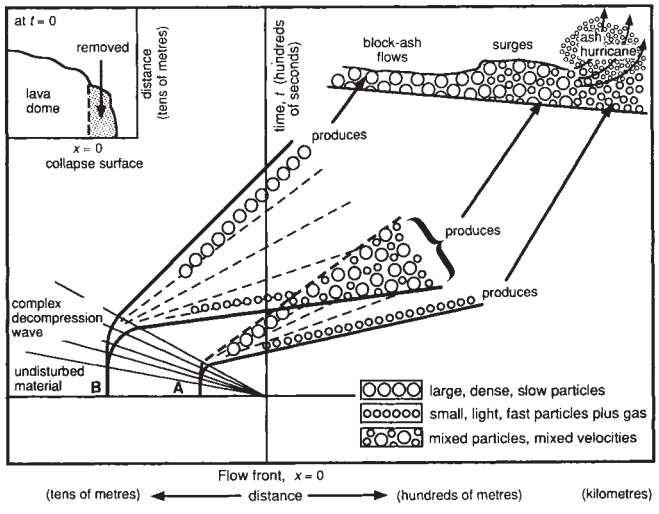

FIG.2 Schematic space–time diagram of the evolution of dome collapse and flow initiation. The slopes of lines radiating from the origin represent relative velocities. The collapse surface migrates from origin A to B.

Received 26 January; accepted 6 May 1993.

1. Nakada, S. Fujii, T. *J. Volcan. geotherm. Res.* **54**, 319–334 (1993).
2. Macdonald, G. A. *Volcanoes* (Prentice Hall, Englewood Cliffs, New Jersey, 1972).
3. Malin, M. C. & Sheridan, M. F. *Science* **217**, 637–639 (1982).
4. Smith, R. L. *Geol. Soc. Am. Bull.* **71**, 795–842 (1960).

5. Sparks, R. S. J., Wilson, L. & Hulme, G. *J. geophys. Res.* **83**, 1727–1739 (1978).
6. Woods, A. W. & Caulfield, C. P. *J. geophys. Res.* **97**, 6699–6712 (1992).
7. Rose, W. I. Jr, Pearson, T. & Bonis, S. *Bull. Volcanol.* **40**, 53–70 (1976).
8. Sato, H., Fujii, T. & Nakada, S. *Nature* **360**, 664–666 (1992).
9. Stith, J. L., Hobbs, P. V. & Radke, L. F. *Geophys. Res. Lett.* **4**, 259–262 (1977).
10. Mellors, R. A., Waitt, R. B. & Swanson, D. A. *Bull. Volcanol.* **50**, 14–25 (1988).
11. Fink, J. H. & Manley, C. R. *IAVCEI Proc. Volcanol.* **1**, 169–179 (1989).
12. Bardintzeff, J. M. *J. Geodynam.* **3**, 303–325 (1985).
13. Kieffer, S. W. *U. S. Geol. Surv. Prof. Pap.* 1250, 379–400 (1982).
14. Sousa, J. & Voight, B. *Geotechnique* **41** (4), 515–538 (1991).
15. Fink, J. H. & Manley, C. R. *Geol. Soc. Am. spec. Pap.* **212**, 77–88 (1987).
16. McBirney, A. R. & Murase, T. A. *Rev. Earth planet. Sci.* **12**, 337–357 (1984).
17. Griffiths, R. W. & Fink, J. H. *J. Fluid Mech.* **252**, 667–702 (1993).
18. Iverson R. *IAVCEI Proc. Volcanol.* **2**, 47–69 (1990).
19. Williams, H. & McBirney, A. R. *Volcanology* (Freeman Cooper, San Francisco, 1979).
20. Anderson, S. W. & Fink, J. H. *IAVCEI Proc. Volcanol.* **2**, 25–46 (1990).
21. Anderson, S. W., Fink, J. H., & Rose, W. I. Jr *Eos* **71**, 1720 (1990).
22. Eichelberger, J. C., Carrigan, C. R., Westrich, H. R. & Price, R. H. *Nature* 323, 598–602 (1986).
23. Manley, C. R. & Fink, J. H. *Geology* **15**, 549–552 (1987).
24. Westrich, H. R., Stockman, H. W. & Eichelberger, J. C. *J. geophys. Res.* **93**, 6503–6511 (1988).
25. Westrich, H. R. & Eichelberger, J. C. *N. M. Bur. Mines Min. Res. Bull.* **131**, 206–291 (1989).
26. Manley, C. R. *J. Volcan. geotherm. Res.* **18**, 224–233 (1992).
27. Dzurisin, D., Denlinger, R. P. & Rosenbaum, J. G. *J. geophys. Res.* **95**, 2763–2780 (1990).
28. Wallis, G. B. *One-dimensional Two-Phase Flow* (McGraw Hill, New York, 1969).
29. Zucrow, M. J. & Hoffman, J. D. *Gas Dynamics*, Vol. 1 (Wiley, New York, 1976).

ACKNOWLEDGEMENTS. We thank Bill Rose for an insightful critique. Research supported by NASA and NSF.

TABLE 1 Electron microprobe analyses

		Spinels			
Oxides (%)	Smectite	1	2	3	4
Na_2O	<0.5	—	—	—	—
MgO	4.8 (0.6)	19.5	20.2	16.0	15.0
Al_2O_3	10.3 (1.1)	22.8	12.0	5.3	3.8
SiO_2	56.6 (1.8)	0.6	1.7	0.7	1.5
K_2O	2.7 (0.9)	—	—	—	—
CaO	2.7 (0.6)	0.4	0.7	0.8	0.9
TiO_2	0.5 (0.1)	0.3	0.6	0.2	<0.1
Cr_2O_3	<0.1	0.2	0.2	1.4	1.0
MnO	<0.1	0.4	0.7	0.8	0.7
FeO	—	3.9	0.6	2.4	0.6
Fe_2O_3	21.5 (1.9)	51.4	59.5	68.5	69.0
NiO	<0.2	1.5	2.5	4.9	6.9
Sum	100.0	101.0	98.7	101.0	99.5

Electron microprobe analyses (in weight %) of the clay matrix (smectite) and spinel crystals in spheroids and fragments recovered from hole 577B-1. The smectite composition is given from the analysis of 30 particles; values in parentheses represent 1σ standard deviation. Most of the spinels (>80%) have composition corresponding to analyses 1 and 2. However, compositions 3 and 4 are also observed. FeO and Fe_2O_3 are calculated assuming the spinels are stoichiometric.

Evidence for a K/T impact event in the Pacific Ocean

E. Robin, L. Froget, C. Jéhanno & R. Rocchia

Centre des Faibles Radioactivités CEA/CNRS, 91190 Gif-sur-Yvette, France

THE chemical, mineralogical and isotopic characteristics of deposits at the Cretaceous/Tertiary (K/T) boundary are suggestive of a large impact event, the prime candidate[1] being the Chicxulub crater in Yucatan, Mexico. Spinel-bearing spherules, which may be associated with such impacts, have been reported[2] at several K/T boundary sites worldwide, but their origin is still uncertain. We have examined the spinel-bearing material recovered from K/T boundary deposits at site 577 in the Pacific Ocean[3] and find two distinct populations of particles: spherules with dendritic spinel textures dispersed throughout the grains and irregularly shaped fragments with spinels essentially confined to the rim. The morphology and composition of the particles are characteristic of melted and partially melted meteoritic ablation debris, but their location is difficult to reconcile with an impact on the Yucatan peninsula, some 10,000 km away. We suggest instead that the spinel-bearing particles at site 577 are derived from the impact of a 2-km asteroid in the Pacific Ocean, and that several accretionary events of this type are required to explain the global distribution of spinel-bearing spherules at the K/T boundary.

At Deep Sea Drilling Program (DSDP) site 577 (32° 26.51′ N and 157° 43.40′ E, on the flank of the Shatsky rise[3]) a complete K/T boundary transition is recorded in a nearly pure carbonate (>95%) sequence[3,4]. The palaeontological boundary here, defined by nannofossil studies[5], coincides with an Ir anomaly[6] and with the occurrence of spinel-bearing spheroids[2,4].

We have looked for such spheroids and other debris at hole 577B-1, in a 523-mg sample collected at level 577B-1-4, 69–71 cm deep[6]. The carbonate fraction was dissolved in 10% acetic acid and the coarse fraction (> 50 μm), weighing ~ 4.2 mg, was irradiated for 72 hours in a flux of 2.3×10^{14} neutrons cm^{-2} s^{-1} from the OSIRIS reactor at Pierre SUE Laboratory (Saclay). The fine fraction (<50 μm), weighing ~ 25.8 mg, and 100 mg of whole-rock sample were also irradiated for 2 hours. These samples and about 100 particles randomly extracted from the coarse fraction were analysed for Ir, Ni, Co, Cr, Sc and rare-earth elements with a high-purity Ge γ-ray detector. Individual particles were then mounted in epoxy and polished for detailed scanning electron microscopy and electron microprobe analysis.

Particles from the coarse fraction were sorted in two populations according to morphology: spherules (Fig. 1*a* and *b*, 80–90% of the particles) and irregular fragments (Fig. 1*d* and *e*, 10–20% of the particles). The spherules from population 1 contain varying amounts of spinels embedded in a clay matrix. The dendritic and skeletal morphologies of the spinels and their uniform distribution throughout the grains are indicative of rapid crystallization from completely melted droplets. The irregular fragments from population 2 are composed of nearly pure clay rimmed with tiny spinels. The existence of a continuous rim of spinels surrounding a core relatively free of these crystals shows that these particles are not parts of broken spherules from population 1, or part of other debris, but are undamaged whole particles which have undergone partial melting. Similar features are observed in cosmic objects such as micrometeorites[7–12] and ablation debris from natural and artificial meteorites[13–15] which have been heated and oxidized in the Earth's atmosphere (Fig. 1*c*, *f*).

X-ray diffraction analysis of a set of spherules indicates that the dominant spinel endmember is magnesioferrite, consistent with the high ferric/ferrous ratio derived from compositional data ($Fe^{3+}/Fe^{2+} > 10$; Table 1). Our chemical analyses of about 100 spinels are consistent with those previously reported[16]: they have high Ni (> 1%) contents, low Ti contents (< 1%) and a high iron oxidation state (Fe^{3+}/Fe total ≈ 99 at%, Table 1). The only process known to form spinels with such a composition is ablation and oxidation of meteoritic debris in the atmosphere[17–20]. Such spinels have also been found in spherules associated with oceanic impact debris from Late Pliocene sediments[21]. The existence of such spinels in nearly all the particles at site 577 supports the view that they mostly derive from ablation in the atmosphere of meteoritic material. As